NONLINEAR CURRENT CONTROL METHOD FOR ACTIVE POWER FILTERS

Marcelo Gradella Villalva*, Milton E. de Oliveira Filho† and Ernesto Ruppert Filho‡
School of Electrical and Computer Engineering
Campinas State University (UNICAMP), Campinas, SP, Brazil
* Email: mvillalv@dsce.fee.unicamp.br
† Email: mfilho@dsce.fee.unicamp.br
‡ Email: ruppert@fee.unicamp.br

***Abstract*— This paper presents a new current control method for active power filters. This method uses nonlinear controllers instead of the traditional linear controllers. This paper demonstrates that the proposed method has good dynamic response. A comparison with the deadbeat current control and the proportional-integral current control shows that the performance of the nonlinear current control method is superior.**

***Keywords*—current control, nonlinear control, active filter**

I. INTRODUCTION

Shunt active filters are widely used in electric systems to compensate harmonic, reactive and zero sequence currents. The shunt active filter is composed basically of a current compensator, a current controller and a power inverter operating as a current source. Figure 1 shows a shunt active power filter schematic diagram. A three-leg voltage source inverter feeds three coupling inductors. The inverter and the inductors L1, L2 and L3 act as a controllable current source. The current controller controls the switches S1-S6 through a closed-loop control which makes the compensation currents i_{ca}, i_{cb} and i_{cc} be injected in the electric system.

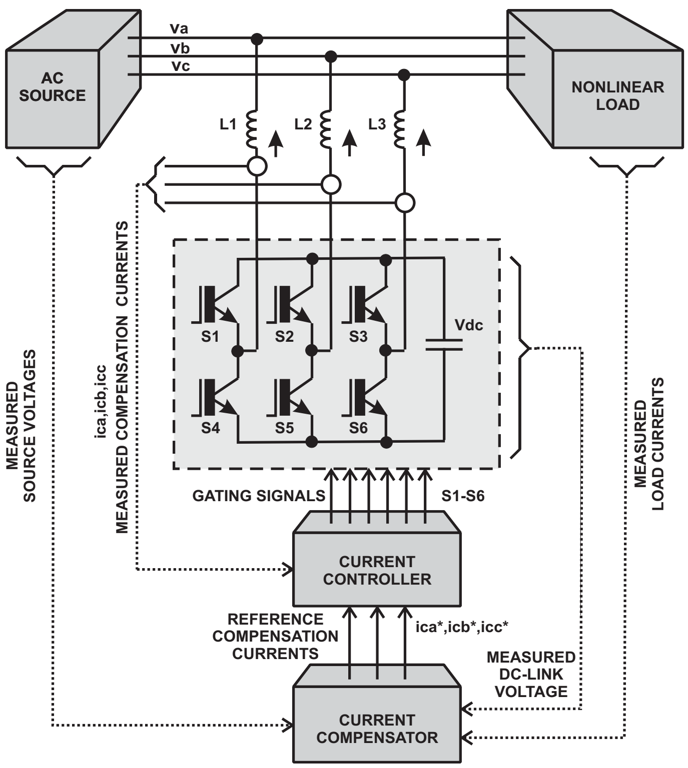

Fig. 1. Three-wire shunt active filter connected to the electric system.

The performance of the whole active filtering system depends on the current control method used. Many techniques of current control have been developed in the past decades. In [1] there is an overview of some of the available current control techniques.

Two widely used techniques are the hysteresis-band current control and the proportional-integral current control with pulse width modulation. The first one is very robust, fast and relatively simple but it does not have a fixed switching frequency. Works like [2]–[4] give detailed information on the hysteresis current control. The second one is also simple but has a lower dynamic response and may present instability problems. However it is the preferred technique in commercial applications due to its constant modulation frequency. Another technique used in commercial applications is the deadbeat control with pulse width modulation. It uses a deadbeat digital controller, which is pointed out by [5] as the most effective digital current control technique for power converters. The drawback of this kind of controller is the inherent time delay introduced by the deadbeat algorithm. This delay can be reduced with some modifications of the deadbeat algorithm, however this decreases the control robustness. These subjects are discussed in [5], [6].

This paper presents a new strategy of current control that can be used in shunt active filters. This new technique is based on a nonlinear controller which has robustness even under modelling uncertainties and disturbance conditions. Nonlinear controllers are used in the control of nonlinear plants. The current control system used in the scheme of figure 1 is ideally linear. However it is subjected to disturbances or variations of parameters and may present a nonlinear behavior which can lead to instability.

The proposed method is validated through a simulation of a three-phase three-wire current controller with space vector pulse width modulation (SVPWM) [7].

II. CURRENT CONTROL WITH NONLINEAR CONTROLLER

In a shunt active filter the current controller must control the active filter line currents. Figure 2 shows the scheme of a current controller. In this scheme there are two reference currents i_α^* and i_β^* which comprise the positive and negative sequence currents injected in the three-phase system by the active filter. The nonlinear controller receives the reference currents and the measured currents and feeds the SVPWM modulator with the reference signals u_α^* and u_β^* in order to obtain the desired currents with the power inverter. This control scheme may be used in four-wire systems with the addition of another controller for the zero sequence current.

Three-phase abc currents and voltages may be transformed into the $\alpha\beta$ system with the $abc-\alpha\beta$ transformation shown in (1).

$$\begin{bmatrix} i_\alpha \\ i_\beta \end{bmatrix} = \sqrt{\frac{2}{3}} \cdot \begin{bmatrix} 1 & -\frac{1}{2} & -\frac{1}{2} \\ 0 & \frac{\sqrt{3}}{2} & -\frac{\sqrt{3}}{2} \end{bmatrix} \cdot \begin{bmatrix} i_a \\ i_b \\ i_c \end{bmatrix} \tag{1}$$

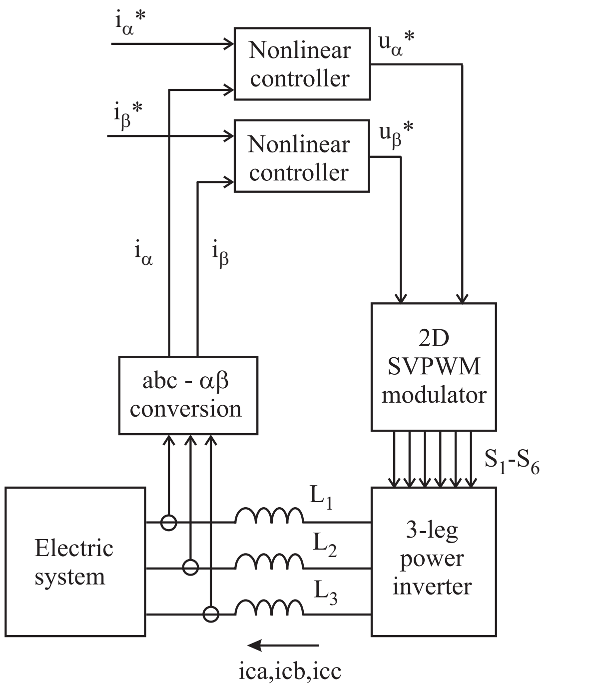

Fig. 2. Current control scheme in a three-wire system with nonlinear controllers.

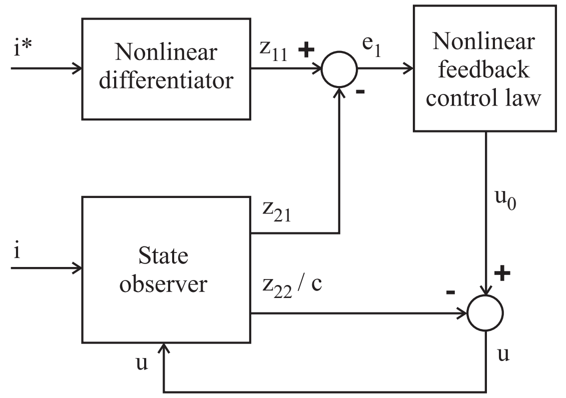

Fig. 3. Nonlinear controller for a first order system.

III. Nonlinear controller

The nonlinear controller used in this research is based on [8]–[10]. This controller provides disturbance compensation even under model mismatches and uncertainties. This kind of controller also provides good dynamic response and negligible overshoot in transient conditions. Simulations made in this research also show that the current control strategy with the studied nonlinear controller can achieve good current tracking and robustness. Several variable adjustments can be modified in order to achieve small error and fast dynamic response. The nonlinear controller is composed of three parts: a nonlinear differentiator, a state observer and a nonlinear feedback control law. In [8]–[10] it is shown that for a first order system a first order nonlinear differentiator and a second order state observer must be used. The current control system can be simplified like a first order plant where a voltage source feeds an inductor and a resistor. This simplification is good enough due to the disturbance rejection capability of the nonlinear controller.

Figure 3 shows the complete scheme of the nonlinear controller for a first order system. The controller of this figure receives two signals i^* and i which are, respectively, the reference current and the measured current. The signal i^* corresponds to the signals i^*_α and i^*_β found in figure 2. The signal i corresponds to the signals i_α and i_β found in figure 2. The output of the controller is u, which corresponds to the signals u^*_α and u^*_β of figure 2.

A. Nonlinear differentiator

The nonlinear differentiator receives the input reference signal and supplies the signal z_{11} to the subtractor which generates the error signal e_1. The derivative of z_{11} is calculated in (2). One integrator is used to obtain z_{11} from $\dot{z}_{11}$.

$$\dot{z}_{11} = -r \cdot f(z_{11} - i^*, \alpha, \delta) \tag{2}$$

The function $f(\cdot)$ is given by (3).

$$f(\epsilon, \alpha, \delta) = \begin{cases} |\epsilon|^\alpha \cdot signal(\epsilon) & , |\epsilon| > \delta \\ \epsilon / \delta^{1-\alpha} & , |\epsilon| \leq \delta \end{cases} \tag{3}$$

The parameters r, α and δ must be correctly chosen in order to achieve fast convergence and small tracking error. The parameter r determines the magnitude of the response obtained with the nonlinear controller. The parameter α is a scaling factor empirically determined which can assume values $\alpha = 1/(2n)$, $n \,\epsilon\, \{1, 2, 4\}$. The parameter δ determines the size of the nonlinear region. It directly affects the tracking error of the nonlinear controller.

B. State Observer

The second order state observer is composed of two integrators which supply the z_{21} and z_{22} signals. The derivatives $\dot{z}_{21}$ and $\dot{z}_{22}$ are calculated in (4).

$$\begin{aligned} \dot{z}_{21} &= z_{22} - g_1(z_{21} - i(t)) + c \cdot u(t) \\ \dot{z}_{22} &= -g_2(z_{21} - i(t)) \end{aligned} \tag{4}$$

The functions $g_1(\cdot)$ and $g_2(\cdot)$ are given by (5).

$$\begin{aligned} g_1(z_{21} - i(t), \alpha, \delta) &= \beta_1 \cdot f(z_{21} - i(t), \alpha, \delta) \\ g_2(z_{21} - i(t), \alpha, \delta) &= \beta_2 \cdot f(z_{21} - i(t), \alpha, \delta) \end{aligned} \tag{5}$$

The parameters β_1 and β_2 affect the convergence speed of the state observer. In general they have the same size of r. The function $f(\cdot)$ is the same seen in (3). The value of the parameter c is generally the inverse of the inductance of the inductors fed by the voltage source inverter. This parameter determines the control effort of the whole control system. If a larger value of c is used the system can oscillate and can present high overshoots. Lower values decrease the dynamic response of the current control system.

C. Nonlinear control law

The nonlinear control law is given by (6). The function $f(\cdot)$ is given by (3). In (6) z_{22} is a disturbance estimation which helps to determine the control signal $u(t)$. It is necessary to correctly adjust k_1, which is a gain constant, in order to obtain a satisfactory system response.

$$\begin{aligned} u_0(t) &= k_1 \cdot f(e_1, \alpha, \delta) \\ u(t) &= u_0(t) - z_{22}/c \end{aligned} \tag{6}$$

IV. Other control methods

This section explains the proportional-integral and the deadbeat current controllers. Both are used in a comparison with the nonlinear controller introduced in this paper.

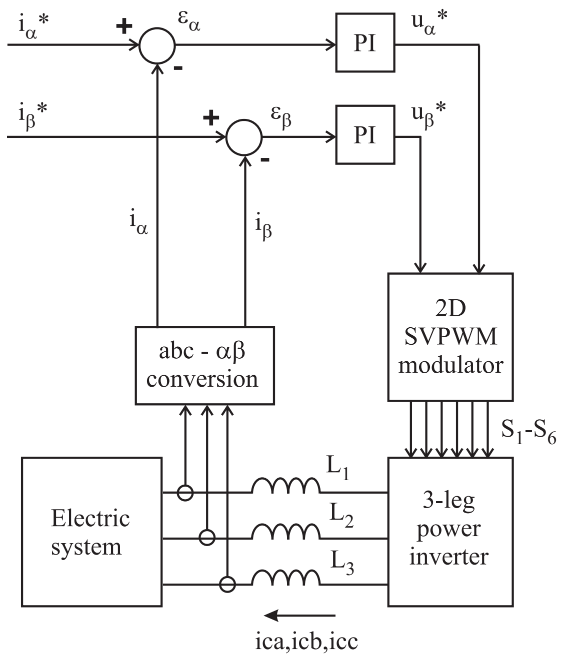

Fig. 4. Current control with PI regulators.

A. Proportional-integral control

This is maybe the most traditional way of achieving current control with power converters at constant switching frequency. Most commercial applications use this kind of controller. Linear proportional-integral (PI) regulators are used together with a pulse width modulator in a scheme identical to that of figure 4. The PI regulators can be easily tuned and implemented in digital form and generally achieve good results.

In the scheme of figure 4 the PI regulators are used to minimize the error signals ε_α and ε_β, which correspond to the differences between the reference currents and the measured currents in the $\alpha\beta$ reference frame. These regulators provide the voltage references u_α^* and u_β^* for the pulse width modulator which drives the power inverter.

B. Deadbeat control

Figure 5 shows the scheme of a deadbeat digital controller which may be used in a current control scheme identical to that of figure 7.

The scheme of figure 5 is derived from equation (7).

$$u(k+1) = f_{pwm}\, L\, [i^*(k) - i(k)] + 2u_s(k) - u(k) \qquad (7)$$

In (7) $u(k+1)$ is the voltage reference of the SVPWM modulator. This reference controls the average phase output voltage of the power inverter. The constant f_{pwm} is the modulation frequency of the pulse width modulator, L is the inductance of the coupling inductor, $i^*(k)$ is the reference current, $i(k)$ is the current measured in the coupling inductor and $u_s(k)$ is the voltage at the coupling point of the inductor with the electric system. The voltage u_s is estimated by equations (8) and (9).

$$u_s(k-1) = u(k-1) + f_{pwm}\, L\, [i(k-1) - i(k)] \qquad (8)$$

$$u_s(k) = (1+\xi)u_s(k-1) - \xi u_s(k-2) \;\; , \;\; 0 \leq \xi \leq 1 \qquad (9)$$

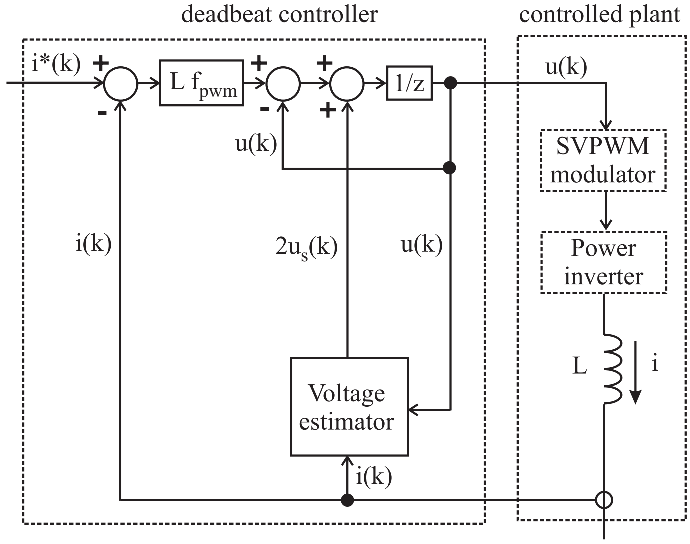

Fig. 5. Deadbeat controller used in current control.

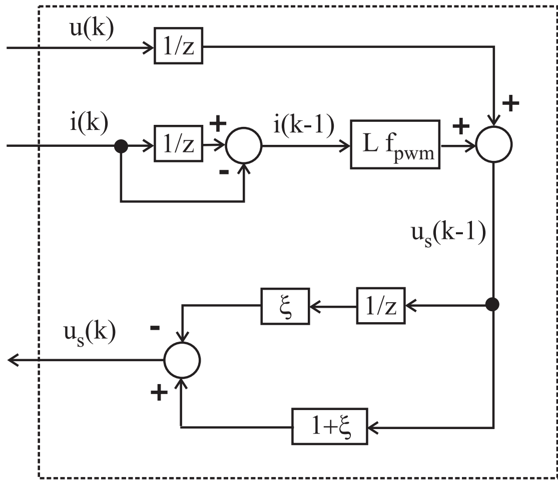

Fig. 6. Voltage estimator.

Figure 6 shows the scheme of the voltage estimator based on equations (8) and (9).

Figure 7 shows a current control scheme using deadbeat controllers. This scheme is similar to that found in figure 2 but with deadbeat controllers instead of nonlinear controllers.

V. Results

A three-phase current control system was simulated with Matlab/Simulink. Three kinds of controllers where used: the deadbeat controller, the proportional-integral controller and the presently studied nonlinear controller. The schemes used in this simulation are those of figure 2, 4 and 7. The reference currents i_α^* and i_β^* of the current controllers are shown in figure 8. The controlled currents i_α and i_β obtained with the simulated controllers are shown in figures 9, 10 and 11. This simulation used $L1 = L2 = L3 = 1.5mH$, $V_{dc} = 400V$ and $R = 0.1\Omega$, where R is the resistance of the inductors.

VI. Conclusion

Disturbance rejection, small tracking error and fast response are very important in current control systems. The proportional-integral control technique requires high gains in order to achieve

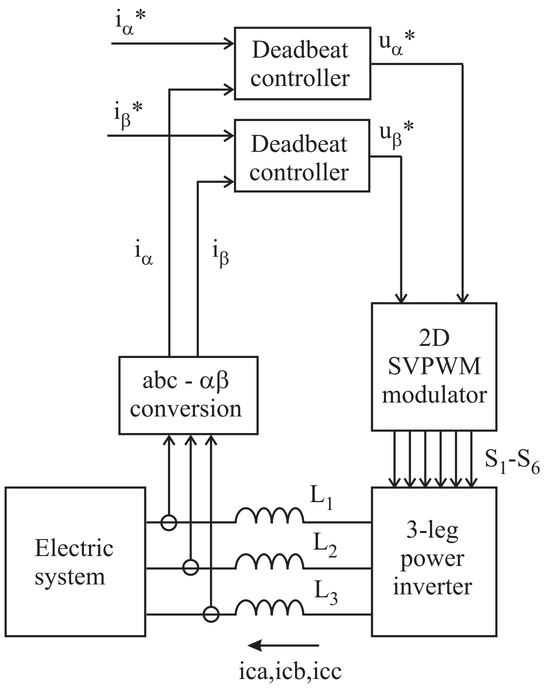

Fig. 7. Current control scheme with deadbeat controllers.

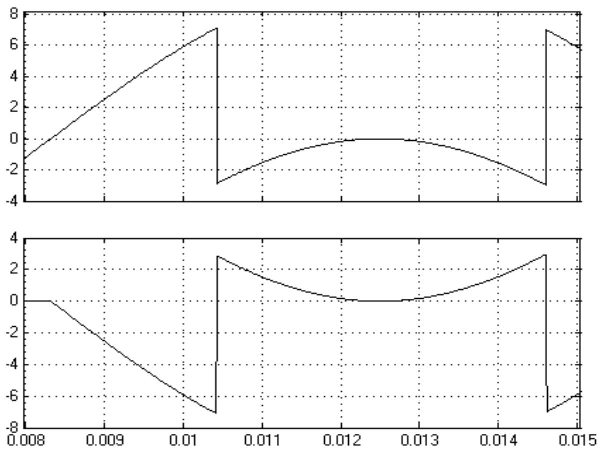

Fig. 8. Reference currents i_α^* and i_β^*. Units are *ampères* and *seconds*.

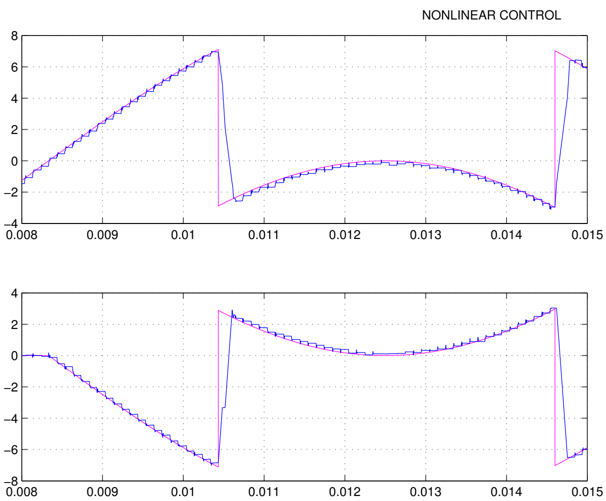

Fig. 9. Currents i_α and i_β obtained with the nonlinear controller. Units are *ampères* and *seconds*.

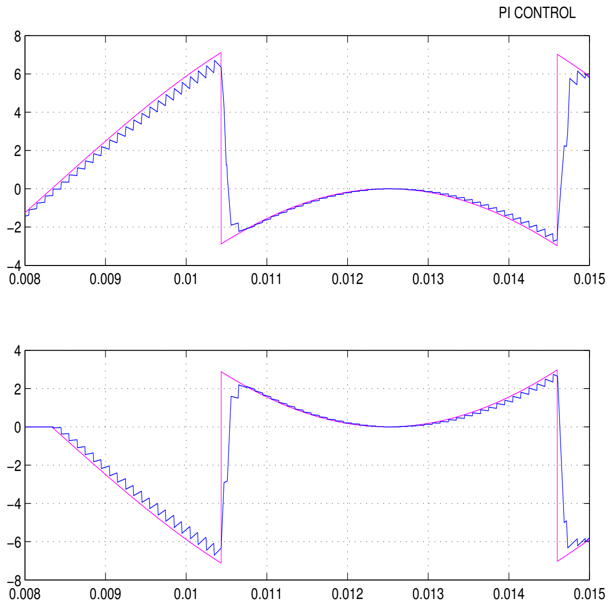

Fig. 10. Currents i_α and i_β obtained with the proportional-integral controller. Units are *ampères* and *seconds*.

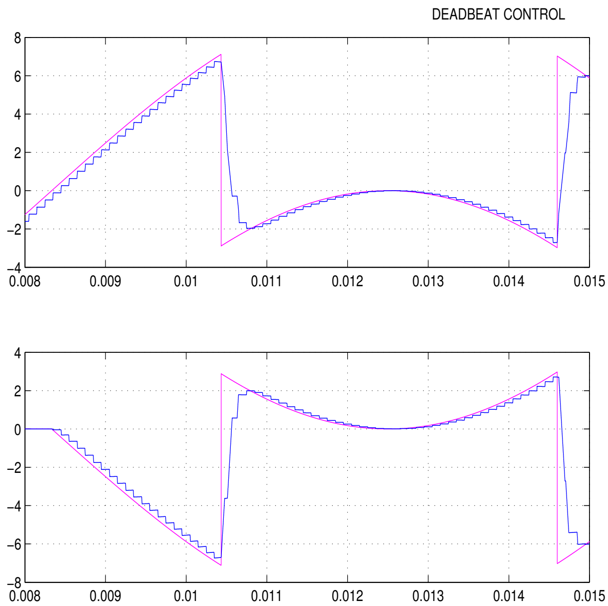

Fig. 11. Currents i_α and i_β obtained with the deadbeat controller. Units are *ampères* and *seconds*.

fast response and small errors, but this can produce current overshoots. The deadbeat current control can achieve good current tracking and fast response, but it is vulnerable to model mismatches, although its robustness against modelling uncertainties can be increased as seen in [6]. The nonlinear controller used in the studied method is robust and the results show that its dynamic response and tracking capability are better than for the current control methods used in the comparison. Although the adjustment of the parameters α, β_1, β_2, r, δ and k_1 can be slightly difficult, the nonlinear control can be an interesting technique for robust and fast current control in active power filters.

ACKNOWLEDGEMENT

The authors are grateful to FAPESP - Fundação de Amparo à Pesquisa do Estado de São Paulo - for the financial support.

REFERENCES

[1] S. Buso, L. Malesani, and P. Mattavelli. Comparison of current control techniques for active filter applications. *IEEE Transactions on Industrial Electronics*, 45(5):722–729, October 1998.

[2] Ching-Tsai Pan and Ting-Yu Chang. An improved hysteresis current controller for reducing switching frequency. *IEEE Transactions on Power Electronics*, 9(1):97–104, January 1994.

[3] Luigi Malesani and Paolo Tenti. A novel hysteresis control method for current-controlled voltage-source pwm inverters with constant modulation frequency. *IEEE Transactions on Industry Applications*, 26(1):88–92, Januray/February 1990.

[4] D. Wuest and F. Jenni. Space vector based current control schemes for voltage source inverters. *Proceedings of the 24th Annual IEEE Power Electronics Specialists Conference, PESC '93*, pages 986–992, June 1993.

[5] L. Malesani, P. Mattavelli, and S. Buso. Dead-beat current control for active filters. *Proceedings of the 24th Annual Conference of the IEEE Industrial Electronics Society*, 3:1859–1864, August/September 1998.

[6] L. Malesani, P. Mattavelli, and S. Buso. Robust dead-beat current control for pwm rectifiers and active filters. *IEEE Transactions on Industry Applications*, 35(3):613–620, May/June 1999.

[7] H. W. van der Broeck, Hans-Christoph Skudelny, and G. Viktor Stanke. Analysis and realization of a pulsewidth modulator based on voltage space vectors. *IEEE Transactions on Industry Applications*, 24(1):140–150, January/February 1988.

[8] Kai Sun, Lipei Huang, and Guang Feng. Speed control of induction motors using a nonlinear auto-disturbance rejection controller. *Proceedings of the 27th Annual Conference of the IEEE Industrial Electronics Society*, 2:1412–1416, November/December 2001.

[9] Guang Feng, Lipei Huang, and Dongqi Zhu. A nonlinear auto-disturbance rejection controller for induction motor. *Proceedings of the 24th Annual Conference of the IEEE Industrial Electronics Society*, 3:1509–1514, August/September 1998.

[10] Guang Feng, Yan-Fei Liu, and Lipei Huang. A new robust control to improve the dynamic performance of induction motors. *Proceedings of the IEEE 32nd Annual Power Electronics Specialists Conference, PESC'01*, 2:778 –783, June 2001.